

## Origin of electron accumulation at wurtzite InN surfaces

I. Mahboob, T. D. Veal, L. F. J. Piper, and C. F. McConville\*

Department of Physics, University of Warwick, Coventry CV4 7AL, United Kingdom

Hai Lu and W. J. Schaff

Department of Electrical and Computer Engineering, Cornell University, Ithaca, New York 14853, USA

J. Furthmüller and F. Bechstedt

Institut für Festkörpertheorie und Theoretische Optik, Friedrich-Schiller-Universität, Max-Wein-Platz 1, D-07743 Jena, Germany

(Received 26 February 2004; published 20 May 2004)

The origin of electron accumulation at wurtzite InN surfaces is explained in terms of the bulk band structure. *Ab initio* calculations of the electronic structure of wurtzite InN reveal an unusually low conduction band minimum at the  $\Gamma$ -point. As a result, the branch point energy,  $E_B$ , which is the crossover point from donor-type to acceptor-type surface states, is located in the conduction band at the  $\Gamma$ -point. This allows donor-type surface states to exist in the conduction band. The donor-type surface states emit their electrons into the conduction band, thus giving rise to electron accumulation at the surface. Experimental measurements, probing the conduction band electron plasma, confirm the existence of electron accumulation at InN surfaces, with a surface Fermi level location in agreement with the predictions of the *ab initio* theory.

DOI: 10.1103/PhysRevB.69.201307

PACS number(s): 71.20.Nr, 73.20.Mf, 73.61.Ey, 73.20.At

Electron accumulation was recently demonstrated to be an inherent property of clean InN(0001) surfaces.<sup>1</sup> Normally, depletion layers occur at III–V semiconductor surfaces, with the surface Fermi level located in the band gap at the  $\Gamma$ -point. This depletion of conduction electrons allows the ionized acceptor-type surface states to be neutralized, giving overall charge neutrality.<sup>2–4</sup> In this article, the physical origin of the electron accumulation at the InN surface is discussed in terms of the calculated *ab initio* bulk electronic structure of wurtzite InN. The electron accumulation is also demonstrated by plasma frequency measurements of the conduction band electrons of InN, combined with carrier profile calculations.

The wurtzite InN band structure is calculated using density functional theory (DFT) within the local density approximation (LDA). A plane-wave expansion of the eigenfunctions and non-normconserving pseudopotentials is implemented in the Vienna *Ab initio* Simulation Package.<sup>5,6</sup> The In 4*d* electrons are treated as valence electrons (dval). This guarantees that the correct structural properties are obtained; the lattice constants are calculated to be  $c = 5.688$  Å and  $a = 3.523$  Å, in agreement with the experimental values for MBE grown films.<sup>7,8</sup> Unfortunately, the conduction and valence bands overlap around the  $\Gamma$ -point in the Brillouin zone (BZ), resulting in a negative fundamental energy gap  $E_g(\text{dval}) = -0.19$  eV. This overlap is mainly a consequence of the overestimation of the *pd* repulsion within DFT-LDA.<sup>9</sup> To avoid this overestimation, another type of pseudopotential has been used, which accounts for self-interaction corrections (SIC) of the 4*d* electrons in the underlying atomic calculation, but freeze the In 4*d* electrons in the core.<sup>10</sup> The self-interaction corrections and the missing *pd* repulsion open up the band gap to  $E_g(\text{SIC}) = 0.58$  eV. Additional quasiparticle corrections were not taken into account in the calculations of the electronic structure that is shown here. The rescaling of the *pd* repulsion practically compensates the

quasiparticle correction, so that the resulting quasiparticle gap (0.81 eV) is only somewhat larger than  $E_g(\text{SIC})$ .<sup>11,12</sup> The electronic structure calculations at the theoretical lattice constants result in the band structure shown in Fig. 1. The SIC bands possess the correct energetical ordering. In this calculation, a computed average high frequency dielectric constant of  $\epsilon(\infty) = 7.16$  is used, very close to the recently obtained experimental values.<sup>12,13</sup> Meanwhile, experimentally, a room temperature band gap of hexagonal InN in the range of 0.60–0.65 eV has been widely confirmed by optical studies.<sup>14–17</sup> The InN band structure revealed by this calculation indicates that the conduction band minimum at the  $\Gamma$ -point is *much* lower than the conduction band edge at other points in *k*-space. Additionally, the optical spectra, computed from the electronic-structure calculations, reveal an absorption edge that is characterized by a steep increase followed by a plateau.<sup>11</sup> This behavior is indicative of a non-

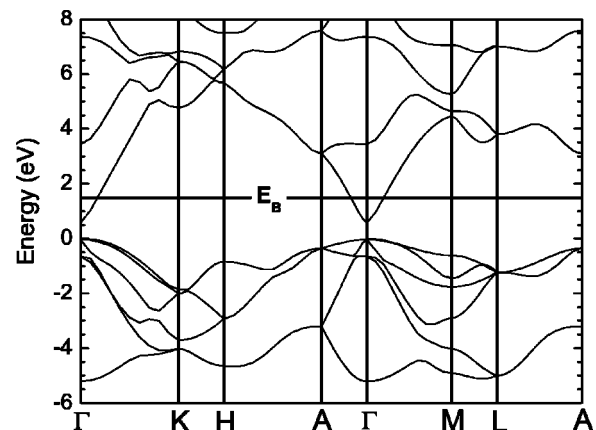


FIG. 1. The wurtzite InN band structure calculated using density functional theory within the local density approximation incorporating self-interaction corrections. The branch-point energy  $E_B$  is shown to be located in the conduction band at the  $\Gamma$ -point.

parabolic conduction band near the  $\Gamma$ -point. This nonparabolicity results in enhanced density of electron states in the conduction band.

The calculated bulk electronic structure can be used to predict the nature of the space-charge layers that occur at wurtzite InN surfaces. The type of surface states present is governed by the position of the branch point energy at the  $\Gamma$ -point. The branch point energy (also known as the charge neutrality level and the Fermi stabilization energy),  $E_B$ , is defined as the cross-over point from states higher in the gap that are mainly of conduction band character (acceptor-type) to states lower in energy that are mainly of valence band character (donor-type).<sup>2</sup> This branch-point energy lies at the center of the band gap (in one dimension) in the complex band structure.<sup>18</sup> Consequently, for the surface states to be neutralized, the surface Fermi level must tend toward the branch point. As a result, the conduction and valence bands bend to generate the space charge required to neutralize the charge generated by the ionized surface states. Whether the surface exhibits electron depletion with upward band bending or accumulation with downward band bending depends on the polarity of the surface states.

The branch point energy is defined as the average midgap energy across the entire BZ;<sup>18</sup> it can be determined by calculating the half-way point between the mean value of the lowest conduction band and the mean value of the highest valence band. This calculation yields a branch point energy that lies  $\sim 1.5$  eV above the valence band maximum and in the conduction band at the  $\Gamma$ -point. Consequently, donor-type surface states exist in the conduction band. These states can acquire positive charge by emitting their electrons into the conduction band. Charge neutrality is then achieved by the accumulation of electrons close to the surface. Clearly, from the *ab initio* band structure, electron accumulation is expected at clean InN surfaces. Conversely, other III–V semiconductors generally exhibit electron depletion.<sup>2–4</sup> This is a consequence of the branch point energy being located in the gap at the  $\Gamma$ -point. Then, for an *n*-type semiconductor, the acceptor-type surface states are occupied. This results in a region close to the surface that is depleted of electrons that can passivate the negatively charged surface states.<sup>3,4</sup> However, accumulation layers will occur at *n*-type InN surfaces because the branch point is located deep in the lowest conduction band at the  $\Gamma$ -point. A similar phenomenon occurs at the InAs surface which also has a low conduction band edge at the  $\Gamma$ -point, and consequently, the branch point is located in the conduction band.<sup>19</sup>

The space-charge layer on the clean InN surface is investigated with high-resolution electron-energy-loss spectroscopy (HREELS). In this technique, low energy probing electrons exchange energy via a Coulombic interaction with polarization fields arising from the collective excitations of both the lattice (phonons) and the electrons in the conduction band (plasmons). By changing the energy of the probing electrons, the entire space-charge region can be surveyed.<sup>20</sup> HREELS is the preferred method to investigate the properties of clean InN surfaces, as unlike other techniques, such as capacitance–voltage profiling, no contacts to the surface are required. Furthermore, rather than probing the entire film,

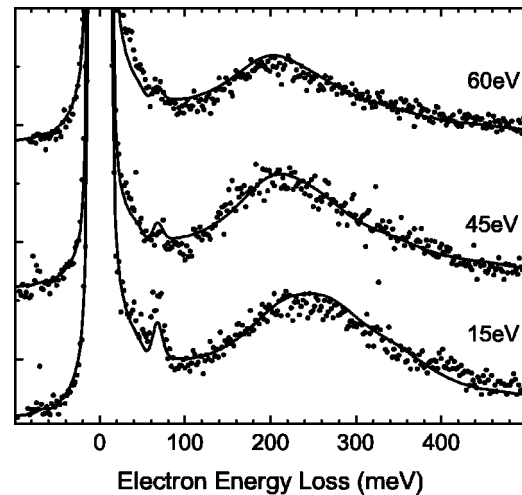


FIG. 2. Specular HREEL spectra recorded at 300 K from an atomic hydrogen cleaned InN(0001) surface with incident electron energies of 15–60 eV (points) and the corresponding semiclassical dielectric theory simulations (solid lines).

HREELS only probes the near-surface space-charge region, allowing this to be distinguished from any charge accumulated at the InN/buffer layer interface.<sup>21</sup> The InN(0001) samples used in this study were grown with unintentional *n*-type doping by migration enhanced molecular beam epitaxy on a GaN buffer layer. Details of the growth can be found elsewhere.<sup>22</sup>

A series of normalized HREEL spectra recorded from the clean InN(0001) surface with a range of probing energies is shown in Fig. 2, along with semi-classical dielectric theory simulations. Two distinct features are observed in the HREEL spectra. The first loss feature at  $\sim 66$  meV is assigned to Fuchs–Kliewer surface phonon excitations.<sup>1</sup> The second loss feature at  $\sim 250$  meV is due to conduction band electron plasmon excitations. The plasmon peak undergoes a  $\sim 40$  meV downward dispersion as the energy of the probing electrons is increased from 15 to 60 eV. This can be understood in terms of a surface layer of higher plasma frequency than that of the bulk and provides direct evidence for the existence of an electron accumulation layer at the InN surface.

The existence of an electron accumulation layer at the InN surface is quantitatively confirmed by simulating the HREEL spectra. The energy exchange between the probing electrons and the polarization field arising from the collective excitations of the free carriers in the conduction band results from the long-ranged Coulomb interaction and can be described by the semiclassical dielectric theory within the methodology of Lambin *et al.*<sup>20,23</sup> Simulations of the spectra are required to obtain the true plasma frequency from the spectra because the observed plasmon peak position is influenced by the band bending, spatial dispersion, and plasmon damping. A five-layer model was required to simulate the HREEL spectra, where each layer has its own frequency- and wave-vector-dependent hydrodynamic dielectric function.<sup>20</sup> A plasma dead layer of 3 Å was required, both to simulate the variation in the phonon peak intensity and approximate the quantum mechanical effect of the surface potential

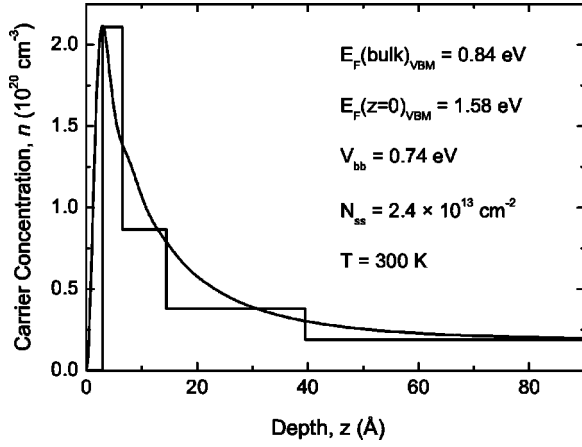


FIG. 3. The layered charge profile used in the HREELS simulations and the corresponding smooth charge profile calculated by solving the Poisson equation within the MTFA.

barrier.<sup>24</sup> Three further layers of enhanced plasma frequency were also needed to reproduce the plasmon tail at high loss energy. Finally, a bulk layer with a plasma frequency of 192 meV was used to obtain the correct plasmon peak position. This layer profile was necessary to reproduce the dispersion of the plasmon peak. The results of the HREELS simulations are shown in Fig. 2, where all the spectra were simulated using the same plasma frequency profile.

Knowledge of the conduction band dispersion relation is required in order to translate the plasma frequencies extracted from HREELS into carrier concentrations. An approximation of the  $\mathbf{k} \cdot \mathbf{p}$  model was utilized to calculate the non-parabolic dispersion of the conduction band.<sup>25</sup> This model was modified for application to heavily doped InN by incorporating the effects of electron–electron interactions and electron-ionized impurity interactions as required in the large wave vector and high Fermi level regime.<sup>25</sup> The interdependence of the plasma frequency,  $\omega_p$ , the carrier concentration,  $n$ , and the effective mass at the Fermi level,  $m_F^*$ , can consequently be calculated by manipulating the conduction band dispersion.<sup>1</sup> These calculations were used to translate the plasma frequencies extracted from the HREELS simulations into carrier concentrations. The resulting conduction electron–depth profile, determined from the HREELS simulations for InN, is presented in Fig. 3. A maximum electron density of  $\sim 2.1 \times 10^{20} \text{ cm}^{-3}$  occurs in the near surface, declining to the bulk carrier concentration of  $1.9 \times 10^{19} \text{ cm}^{-3}$ . This analysis clearly confirms the presence of an intrinsic electron accumulation layer on the clean InN surface.

In order to obtain information about the space-charge layer parameters, the layered charge profiles used in the HREELS simulations can be compared with calculated smooth charge profiles. This enables the amount of band bending, the surface Fermi level, and the surface state density to be determined. Charge profiles were calculated by solving Poisson’s equation within the modified Thomas–Fermi approximation (MTFA). A trial potential,  $V(z)$ , which is a solution of the Poisson equation,

$$\frac{d^2V(z)}{dz^2} = \frac{e}{\epsilon_0\epsilon(0)} [N_D^+ - n(z)], \quad (1)$$

where  $N_D^+$  is the bulk donor density, is used to solve

$$n(z) = \frac{1}{8\pi^2} \left( \frac{2m_0^*}{\hbar^2} \right)^{3/2} \int_0^\infty \frac{E^{1/2} \left( 1 + \frac{E}{E_g} \right)^{1/2} \left( 1 + \frac{2E}{E_g} \right)}{1 + \exp[(E - E_F + V(z))/k_B T]} \times \left( 1 - \text{sinc} \left[ \frac{2z}{L} \left( \frac{E}{k_B T} \right)^{1/2} \left( 1 + \frac{E}{E_g} \right)^{1/2} \right] \right) dE \quad (2)$$

to obtain a charge distribution,  $n(z)$ , with the boundary condition,  $V(z)$  and  $dV(z)/dz \rightarrow 0$  as  $z \rightarrow \infty$ , where  $L$  is the Fermi length. The calculated potential that satisfies the boundary conditions was then used to calculate the surface state density according to

$$N_{ss} = \frac{\epsilon_0\epsilon(0)}{e} \left. \frac{dV(z)}{dz} \right|_{z=0}. \quad (3)$$

The MTFA is an alternative to the self-consistent solution of the Poisson and Schrödinger equations for calculating realistic smooth charge profiles. Without recourse to a modified Schrödinger equation, the MTFA enables the straightforward inclusion of the nonparabolicity of the conduction band,<sup>25</sup> which results in a significantly larger charge accumulation because of the increased density of states higher in the conduction band.<sup>25</sup> It also allows the effects of the surface potential barrier to be included in the calculations with a correction factor, which approximates the interference between incoming and reflected electron waves that smoothly reduces the charge,  $n(z)$ , to zero at the surface.<sup>24</sup> The smooth charge profile that most closely resembles the HREELS simulation profile is shown in Fig. 3. This charge profile calculation yields a surface state density,  $N_{ss}$ , of  $\sim 2.4 (\pm 0.2) \times 10^{13} \text{ cm}^{-2}$ , giving rise to an electric field of  $4.6 \times 10^8 \text{ Vm}^{-1}$  at the surface and band bending,  $V_{bb}$ , of  $\sim 0.74 \text{ eV}$ . As a result of this band bending, the surface Fermi level is located  $\sim 1.58 \pm 0.10 \text{ eV}$  above the valence band maximum. The uncertainties given for the values of surface state density and the Fermi levels is due to the uncertainty in determining the plasma frequency profile from the dielectric theory simulations. The values of  $N_{ss}$  and the Fermi levels are reported for an intrinsic band gap of 0.642 eV at 300 K, which has been determined for the samples used here by previous transmission and photoluminescence spectroscopy studies.<sup>15</sup> This analysis reveals that the Fermi level is located close to the branch point energy of 1.5 eV above the valence maximum as determined from the *ab initio* calculations. Consequently, the donor-type surface states can be partially unoccupied, giving rise to the electron accumulation. Further theoretical and experimental studies, such as *ab initio* calculations and angle-resolved photoemission spectroscopy of the electronic structure of the InN(0001)-(1 × 1) surface, are required to determine the physical nature of these surface states. In the case of polar InAs surfaces, this approach was able to rule out regular surface states as the

cause of electron accumulation and it was concluded that the surface states are native defects.<sup>26</sup>

The *ab initio* calculations of the InN electronic structure reveal an unusually low conduction band minimum at the  $\Gamma$ -point. This enables donor-type surface states to exist in the conduction band. These surface states become ionized by

emitting their electrons into the conduction band. This manifests itself as a surface electron accumulation layer that is required to neutralize the positively charged surface states. The existence of the accumulation is experimentally confirmed by plasma frequency measurements of the conduction band electron plasma.

\*Electronic address: C.F.McConville@warwick.ac.uk

<sup>1</sup>I. Mahboob, T.D. Veal, C.F. McConville, H. Lu, and W.J. Schaff, *Phys. Rev. Lett.* **92**, 036804 (2004).

<sup>2</sup>H. Lüth, *Surfaces and Interfaces of Solid Materials* (Springer, Berlin, 1995).

<sup>3</sup>R. Matz and H. Lüth, *Phys. Rev. Lett.* **46**, 500 (1981).

<sup>4</sup>A. Ritz and H. Lüth, *Phys. Rev. Lett.* **52**, 1242 (1984).

<sup>5</sup>G. Kresse and J. Furthmüller, *Comput. Mater. Sci.* **6**, 15 (1996).

<sup>6</sup>G. Kresse and J. Furthmüller, *Phys. Rev. B* **54**, 11169 (1996).

<sup>7</sup>V.Y. Davydov, A.A. Klochikhin, R.P. Seisyan, V.V. Emtsev, S.V. Ivanov, F. Bechstedt, J. Furthmüller, H. Harima, A.V. Mudryi, J. Aderhold *et al.*, *Phys. Status Solidi B* **229**, R1 (2002).

<sup>8</sup>V. Cimalla, C. Förster, G. Kittler, I. Cimalla, R. Kosiba, G. Ecke, O. Ambacher, R. Goldhahn, S. Shokhovets, A. Georgakilas *et al.*, *Physica Status Solidi C* **0**, 2818 (2003).

<sup>9</sup>F. Bechstedt and J. Furthmüller, *J. Cryst. Growth* **246**, 315 (2002).

<sup>10</sup>M.M. Rieger and P. Vogl, *Phys. Rev. B* **52**, 16567 (1995).

<sup>11</sup>F. Bechstedt, J. Furthmüller, M. Ferhat, L.K. Teles, L.M.R. Scolfaro, J.R. Leite, V.Y. Davydov, O. Ambacher, and R. Goldhahn, *Phys. Status Solidi A* **195**, 628 (2003).

<sup>12</sup>R. Goldhahn, S. Shokhovets, V. Cimalla, L. Spiess, G. Ecke, O. Ambacher, J. Furthmüller, F. Bechstedt, H. Lu, and W. Schaff, *Mater. Res. Soc. Symp. Proc.* **743**, L5.9.1 (2003).

<sup>13</sup>A. Kasic, M. Schubert, Y. Saito, Y. Nanishi, and G. Wagner, *Phys. Rev. B* **65**, 115206 (2002).

<sup>14</sup>M. Higashiwaki, T. Inushima, and T. Matsui, *Phys. Status Solidi B* **240**, 417 (2003).

<sup>15</sup>J. Wu, W. Walukiewicz, W. Shan, K.M. Yu, J.W. Ager III, S.X. Li, E.E. Haller, H. Lu, and W.J. Schaff, *J. Appl. Phys.* **94**, 4457 (2003).

<sup>16</sup>O.K. Semchinova, J. Aderhold, J. Graul, A. Filimonov, and H. Neff, *Appl. Phys. Lett.* **83**, 5440 (2003).

<sup>17</sup>S.X. Li, J. Wu, E.E. Haller, W. Walukiewicz, W. Shan, H. Lu, and W.J. Schaff, *Appl. Phys. Lett.* **83**, 4963 (2003).

<sup>18</sup>J. Tersoff, *Phys. Rev. B* **32**, 6968 (1985).

<sup>19</sup>M. Noguchi, K. Hirakawa, and T. Ikoma, *Phys. Rev. Lett.* **66**, 2243 (1991).

<sup>20</sup>T.D. Veal and C.F. McConville, *Phys. Rev. B* **64**, 085311 (2001).

<sup>21</sup>H. Lu, W.J. Schaff, L.F. Eastman, and C.E. Stutz, *Appl. Phys. Lett.* **82**, 1736 (2003).

<sup>22</sup>H. Lu, W.J. Schaff, J. Hwang, H. Wu, W. Yeo, A. Pharkya, and L.F. Eastman, *Appl. Phys. Lett.* **77**, 2548 (2000).

<sup>23</sup>Ph. Lambin, J.P. Vigneron, and A.A. Lucas, *Phys. Rev. B* **32**, 8203 (1985).

<sup>24</sup>J.P. Zöllner, H. Übensee, G. Paasch, T. Fiedler, and G. Gobsch, *Phys. Status Solidi B* **134**, 837 (1986).

<sup>25</sup>J. Wu, W. Walukiewicz, W. Shan, K.M. Yu, J.W. Ager III, E.E. Haller, H. Lu, and W.J. Schaff, *Phys. Rev. B* **66**, 201403 (2002).

<sup>26</sup>L.Ö. Olsson, C.B.M. Andersson, M.C. Håkansson, J. Kanski, L. Ilver, and U.O. Karlsson, *Phys. Rev. Lett.* **76**, 3626 (1996), and references therein.